Appl. Phys. B 80, 581–585 (2005)
DOI: 10.1007/s00340-005-1746-0

**Applied Physics B**
**Lasers and Optics**

YONGQI FU[1,2,✉]
N.K.A. BRYAN[1,2]

# Investigation of physical properties of quartz after focused ion beam bombardment

[1]Innovation in Manufacturing Systems and Technology (IMST) Program, Singapore–Massachusetts Institute of Technology (MIT) Alliance, 50 Nanyang Avenue, Singapore 639798, Singapore
[2]School of Mechanical and Production Engineering, Nanyang Technological University, 50 Nanyang Avenue, Singapore 639798, Singapore

**Received: 18 October 2004 /**
**Revised version: 13 December 2004**
**Published online: 16 February 2005 •**


**ABSTRACT** Optical properties (transmission and refractive index) and phase change (from amorphous to crystal) of a commonly used glass, quartz, were investigated before and after focused ion beam (FIB) bombardment with ion energy from 30 to 50 keV. We found different influences of FIB bombardment on the optical properties and chemical structure of the quartz in the wavelength region of visible and near infrared, respectively. The quartz still can be used in the infrared wavelength for conventional optical applications. As an application example, an array of diffractive optical elements (DOEs) was directly fabricated on the quartz by the FIB milling. The measured diffraction efficiency of the DOEs is 83.5%, which is acceptable for practical use.

**PACS** 07.85.Nc; 07.85.Jy; 07.60.Hv; 78.20-e

## 1 Introduction

Quartz (fused silica) is a useful optical material with its advantages of wide transmission band, high melting temperature, and high resilience to hostile environments, and bio-compatibility, which makes it appealing and promising for optical system usage. It is commonly used in micro-optical systems for bio-chemical analysis and optical communication. In our projects, we use the quartz as the substrate material to fabricate micro-optical elements by use of focused ion beam (FIB) direct milling or deposition [1–6]. FIB milling or deposition is a one-step fabrication. Any pattern transfer is not necessary. It is especially suitable for the localized one-step fabrication in the microsystems. However, the FIB process has a side effect, $Ga^+$ implantation. More or less $Ga^+$ will be implanted under the sample surface. Penetration depth strongly depends on the ion energy. It will cause variation of physical properties of the quartz. Few technical papers have been found that report on the variation of physical properties after the FIB processing till now.

✉ E-mail: yqfu@ntu.edu.sg

In this paper, we investigated the variation of physical properties of the quartz by means of the FIB milling. Different ways were used to characterize the quartz before and after the FIB processing. As an application example, we fabricated a $10 \times 10$ array of the micro-diffractive optical element (DOEs) with a diameter of 65 μm on the quartz. It is a direct fabrication method with features of one-step, isotropic etching, and non-selectivity of the material. Optical properties of the quartz before and after FIBM were discussed in detail in the view of the micro-DOEs application.

## 2 Experimental setup

The milling experiments were carried out using our FIB machine (Micrion 9500EX dual beam system) with an ion source of liquid gallium, integrated with a scanning electron microscope (SEM), energy dispersion X-ray spectrometer (EDX) facilities and gas assistant etching (GAE) functions. This machine uses a focused $Ga^+$ ion beam with an energy ranging from 5 to 50 keV, a probe current ranging from 4 pA to 19.7 nA, and a beam limiting aperture size ranging from 25 to 350 μm. For the smallest beam currents, the beam can be focused down to as small as 5 nm in diameter at full width and half maximum (FWHM). The milling process is performed under programming control, by means of varying the ion dose for different relief depth. A UV–Vis transmittance spectrum (UV–Vis spectrophotometer) was used to measure transmittance of the quartz before and after FIB processing. The smallest illumination area required for measurement is $5 \times 5\ mm^2$. The area is quite large for FIB milling (very time consuming for our FIB machine). The maximum milling area of our machine is $1 \times 1\ mm^2$. We have to cover the area of $5 \times 5\ mm^2$ by milling a square pattern (the area for each pattern is $650 \times 650\ \mu m^2$) with $10 \times 10$ array. The necessity of an array causes degradation of surface roughness uniformity, which will affect transmittance to a certain extent.

## 3 Results and discussions

### 3.1 *Phase change before and after FIB processing*

Our quartz samples are amorphous quartz. We paid attention to the phase change between crystalline and

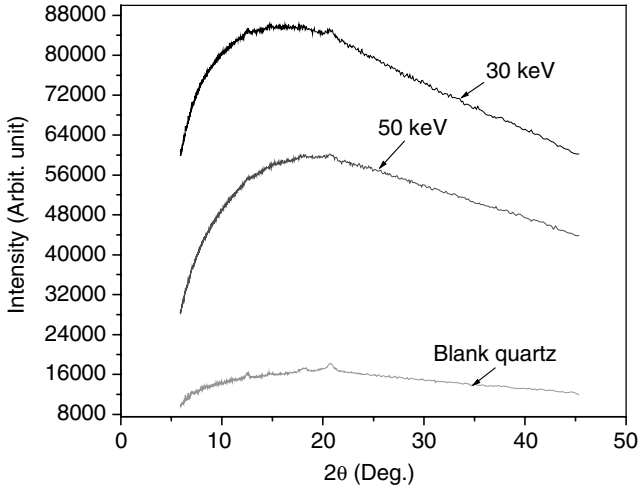


**FIGURE 1** XRD results for the quartz bombed by the ion beam with 30 and 50 keV, respectively

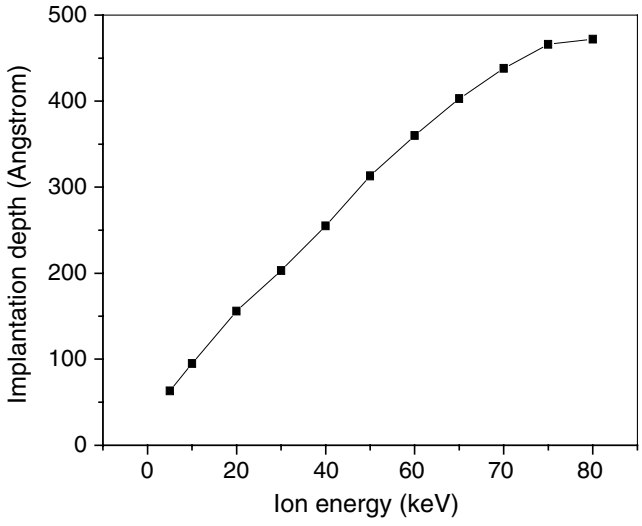


**FIGURE 3** Simulation results of ion implantation depth vs. ion energy in direction of longitudinal. The relationship between implantation depth and ion energy is linear in the range from 5 to 80 keV

amorphous (it will influence the future optical performance of the quartz made optical devices) after the FIB bombardment. Today, the most accepted methods for analysis of quartz are X-ray diffraction (XRD) and infrared spectroscopy (IR). We used XRD for the analysis of quartz. Figure 1 shows the XRD spectrum before (blank quartz) and after the FIB bombardment with ion energy of 30 and 50 keV, respectively. It can be seen that not any apparent crystalline related sharp peaks were found for the cases of before and after the FIB bombardment. The locations of the crest of convex curves are nearly the same for the different cases. Although a strong change in the intensity of the XRD spectra can be detected, as seen in Fig. 1, which might be due to measuring time and not be important. Therefore, we can draw a conclusion that no phase change occurs during the FIB bombardment, even for the maximum energy of 50 keV used. It may be the reason that temperature rise caused during the FIB bombing on the surface of the quartz is lower. Figure 2 is the simulation results

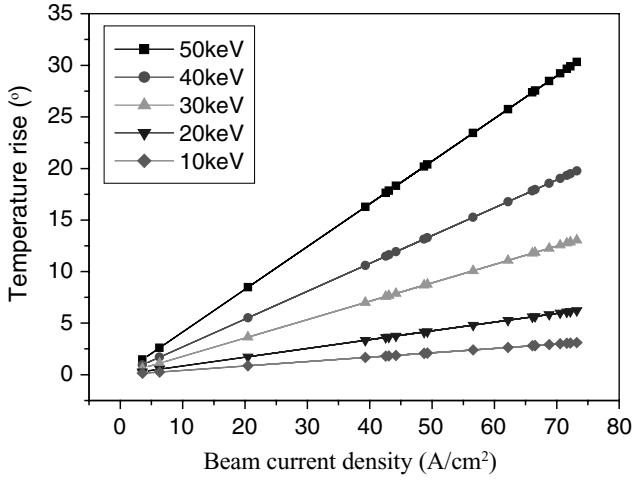


**FIGURE 2** Simulated temperature rise vs. ion beam current density for quartz bombed with different ion energy. The maximum temperature rise can be 32°C for the ion energy and beam current density of 50 keV and 75 A/cm$^2$, respectively

of the temperature rise vs. beam current density for different ion energies in terms of John's model in Ref. [7]. It can be seen that the maximum temperature rise is 32°C for the ion energy and beam current density of 50 keV and 75 A/cm$^2$, respectively, and is only several degrees for the smaller beam current (in this case, the FIB has a higher resolution). This temperature rise is insufficient to affect thermal stability of the quartz.

### 3.2 *Ga$^+$ implantation after FIB bombardment*

Figure 3 is a simulated result of implanted depth of Ga$^+$ vs. different ion energy by use of commonly used ion beam simulation software (TRIM 2000 [7]). It can be seen that the implantation depth for the quartz-like surface is 208, 257, and 313 Å for the ion energy of 30, 40, and 50 keV, respectively. The percentage of the implanted Ga$^+$ measured by the electron dispersion X-ray spectrometer (EDX) is 9.8, 12.3 and 15% for the ion energy of 30, 40, and 50 keV, respectively, as shown in Fig. 4. Penetration of the X-ray is around 30 nm under sample surface, that just match with the implantation depth of the Ga$^+$ at 50 keV.

### 3.3 *Optical properties before and after FIB bombardment*

More or less Ga$^+$ implantation may occur during FIB bombardment, which may affect the transmission of the quartz due to Ga$^+$ implanted on the surface of the quartz, especially for a visible wavelength. Figure 5 shows a comparison of the transmittance of the quartz measured before and after FIB processing as determined using UV–Vis transmittance spectroscopy (UV–Vis spectrophotometer HP8453). It can be seen that the transmission was decreased with increasing ion energy. Variation is small before and after the FIB bombardment with ion energy of 30 keV in the near infrared region. Even for the bombardment with 50 keV, transmission is still

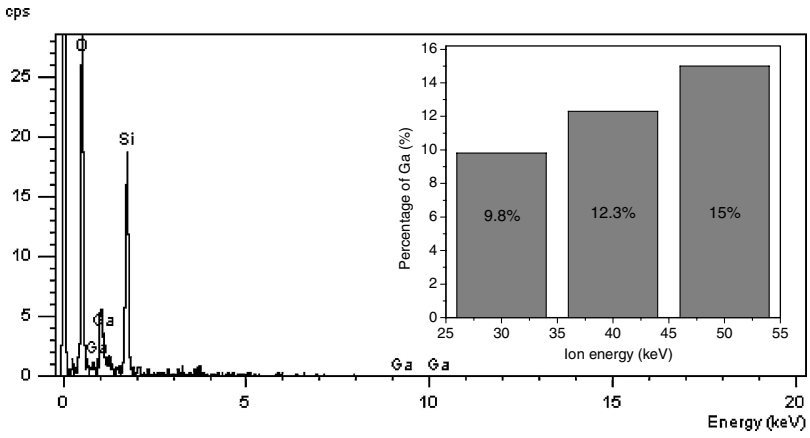


**FIGURE 4** Results of chemical elements analyzed by EDX. The percentage of Ga implanted in the quartzes was 9.8, 12.3, and 15% for the ion energy of 30, 40 and 50 keV, respectively

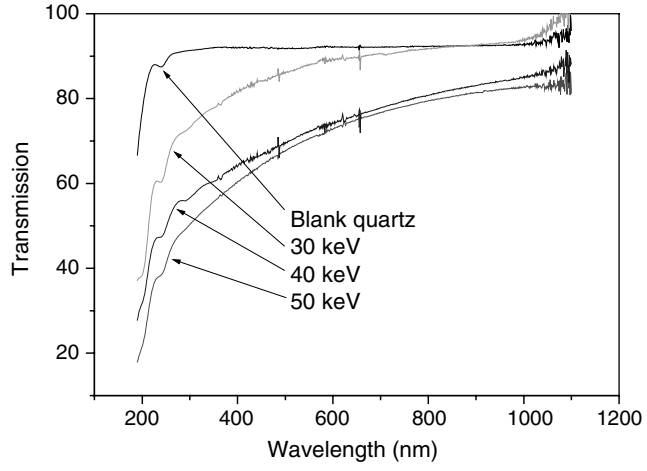


**FIGURE 5** Transmission of the quartz vs. wavelength before and after ion beam bombardment with different ion energy ranging from 30 to 50 keV

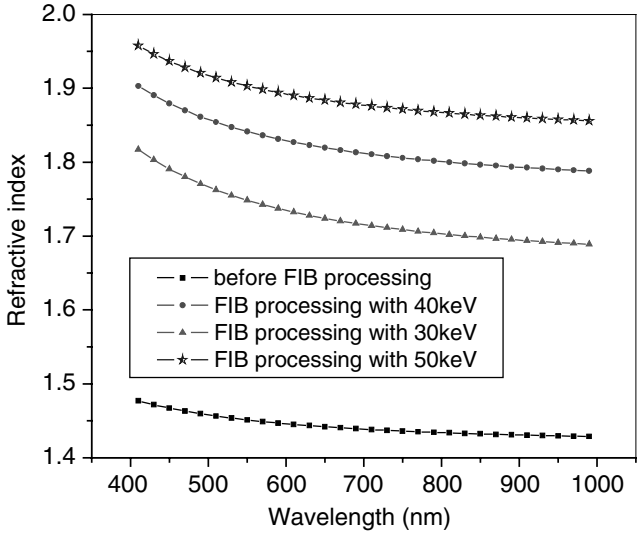


**FIGURE 6** Refractive index of the quartz vs. wavelength before and after ion beam bombardment with different ion energy ranging from 30 to 50 keV

above 70% for the wavelength larger than 600 nm. Transmission is constant with a value of ∼85% for wavelength larger than 900 nm and can meet requirement of conventional optical system. The quartz after the FIB milling is more suitable for the applications of the micro-optical elements working in the near infrared wavelength than that of the visible wavelength.

Figure 6 shows the relationship of refractive index versus wavelength before and after the FIB milling process measured with an ellipsometer (Mizojiri Kogaku) equipped with He–Ne laser. For the bulk material of fused silica, measurement of extinction coefficient $k$ is strongly affected by the presence of water or OH absorption in the samples makes the determination of the intrinsic $k$ values extremely difficult for the wavelength in the range $3.7 \geq \lambda \geq 0.21$ [8]. Thus no $k$ values were given in this figure. It can be seen that the refractive index increased around 0.5 after the FIB milling. The larger the ion energy used, the higher the refractive index will be. The increment after the FIB milling is caused due to $Ga^+$ implantation with different ion energy. In the theoretical point of view, these physical phenomena may be explained as follows: The dielectric constant $\varepsilon$ is the square of the complex refractive index, which determines the optical properties of a given material. According to the classical Drude model, the real and imagery parts of the complex refractive index are obtained as [9]

$$\varepsilon = \left(\varepsilon_1^2 + \varepsilon_2^2\right)^{1/2} = n^2 + k^2, \tag{1}$$

$$n = [(\varepsilon + \varepsilon_1)/2]^{1/2}, \tag{2}$$

$$k = \varepsilon_2/2n = [(\varepsilon - \varepsilon_1)/2]^{1/2}, \tag{3}$$

where $\varepsilon_1$, $\varepsilon_2$ is the real part and imaginary part of the dielectric constant, respectively, $n$ and $k$ the real part and imaginary part of the complex refractive index, respectively, $k$ also called extinction coefficient.

For the quartz surface implanted with metal ions, the dielectric constant function with the metal can be expressed as [10]

$$\varepsilon_{\mathrm{M}} = 1 - \frac{\omega_{\mathrm{p}}^2}{\omega^2 + i\omega\gamma}, \tag{4}$$

$$\omega_{\mathrm{p}}^2 = 4\pi n_{\mathrm{e}} e^2 / m_{\mathrm{n}} \varepsilon_{\infty}, \tag{5}$$

in which $\omega_{\mathrm{p}}$ is the plasmon/resonance frequency, and $\gamma$ the relaxation frequency of oscillation, depending on the mean free path of electrons, $\omega$ the frequency of free electron oscillation, $n_{\mathrm{e}}$ the free-carrier density, $\varepsilon_{\infty}$ the high-frequency lattice

dielectric constant, $m_n$ the ratio of the dielectric functions $\varepsilon_M/\varepsilon_I$ of the metal and insulating matrix.

In the case of inhomogeneous sample, such as implanted films or ion beam mixed single layers, the transmission can be defined from a Lambert-Beer law [10]:

$$T = \exp(-kt) = \exp(-\sigma N t), \tag{6}$$

where $\sigma$ is the extinction cross section of clusters, $N$ their number density per unit volume, $t$ the thickness of the composite. With the ion energy increasing, the implanted depth on the surface layer is deeper and deeper. It causes the frequency of free electron oscillation $\omega$ becomes higher and higher. It can be known from Eqs. 4 and 2 that $\varepsilon_M$ will increase accordingly, and refractive index $n$ also increases consequently in this case.

For the wavelength, $\lambda \geq 0.6\,\mu m$, it is the region of low absorption. The measured absorption dominated by the presence of OH impurity bands [8]. The implanted $Ga^+$ has limited influence on the transmission of the ion-bombed quartz. Therefore, the difference of transmission curves for different ion energies is smaller in this region compared with that of violet region. For the implantation with metal ions, e.g., $Ga^+$, $Ag^+$, and $Au^+$ etc., the strong and narrow resonance of clusters in the ion beam mixed sample is strengthened by their interaction [10]. This resonance causes an intense increase of optical density (OD) or degradation of transmission in the region of $\lambda < 0.6\,\mu m$, especially in the violet wavelength region. Garia's model predicts the narrowing of the resonance when the contribution to the local polarization from neighboring clusters is positive and much stronger than that from the effective medium due to a particular arrangement of the metal clusters [11, 12]. It was supported by the variation of the resonance width and strength as a function of the distribution of cluster sizes during the mixing process. It also can be explained combining Eq. 6 for the region of $\lambda < 0.6\,\mu m$. With increasing of the ion energy, the range of the implanted ions increases as well. It leads to the larger extinction cross section of the clusters [11], which can degrade the transmission.

The increased refractive index is still usable for the conventional optical system. Numerical aperture of the designed lenses can be improved due to the higher refractive index. In this case, the lens should be designed in terms of the modified refractive index by the Ga ion beam for the corresponding designed wavelength.

We can draw the conclusion that the thermal characteristics of the quartz are stable during the FIB bombardment process because it is a pure physical colliding process between the $Ga^+$ and atoms of the substrate materials with near room temperature. The side-effect—$Ga^+$ implantation at the ion energy of 50 keV is insufficient to affect the transmission of the quartz in the infrared region.

## 4 Application example

As an application example, we fabricated a $10 \times 10$ array of diffractive optical element with six rings on the quartz. Diffraction order of $+1$ was selected as the main diffraction order. The relief accuracy is affected by the beam spot size and pixel overlap during the raster scan. The relief accuracy is deteriorated by the use of larger beam spot size and smaller pixel overlap. Considering the default discrete step size of 0.5 μm, we use the 100-nm beam spot size, 50 keV ion energy, and 60% overlap. Comparing the effects of height error and lateral error on the relief accuracy, we find that the lateral error is prominent. Because of line broadening effect caused by the wing of Gaussian distribution of the ion beam, the actual milled linewidth is larger than the designed size (line broadening). Considering this, the defined linewidth should be less than the designed size. The real value depends on the chosen beam spot size, beam current density and calibration of the ion dose. It takes ∼30 min to fabricate a single micro-DOEs using the FIB method.

The relief accuracy is determined by the beam spot size and overlapping of pixels during the raster scan. The larger the beam spot size and the smaller the overlap, the worse the relief accuracy will be. Considering the interline step of 0.5 μm, we chose a 100-nm beam spot size and 60% overlap for our processes.

Figure 7 shows a SEM micrograph showing the fabricated DOEs. We utilized an AFM (Nanoscope model III A from Digital Instruments) to analyze the surface roughness before and after FIB milling. The scanner was calibrated with a 160 nm height standard. Probing a $1 \times 1\,\mu m^2$ region, average roughness, *Ra*, are 2.1 and 2.5 nm for the 1.5 μm thick quartz before and after FIB milling M, respectively.

In order to evaluate the optical performance of the fabricated element, the diffraction efficiency of the DOEs was measured using a Ti: Sapphire laser (operating wavelength of 800 nm) with a collimation lens, and a photodetector (InGaAs), which provided a value of 83.5% that is acceptable for conventional use.

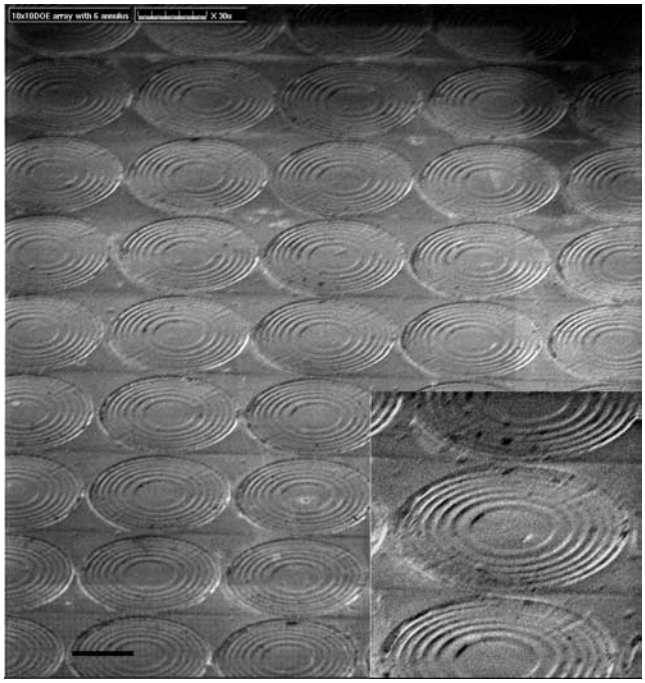

**FIGURE 7** Application example: SEM micrograph of an array of $10 \times 10$ micro-diffractive lens with six annulus, and designed diameter and focal length of 67 and 125 μm, respectively, at working wavelength of 633 nm. *Inset* is zoom-in image. The scale bar is 30 μm. The ion energy used for the milling is 50 keV

## 5 Summary

In summary, fabrication of the micro-DOEs array on the quartz by use of the FIB milling is valid. The surface roughness after the FIB milling is suitable for normal optical applications. Few phase changes occur between the amorphous and the crystal of the quartz after the FIB milling. The influence of the FIB milling on the transmission and the refractive index of the quartz is low for the wavelength of near infrared. Transmission is still above 70% even in the visible wavelength. The technique is more suitable for the fabrication of DOEs working in infrared optical systems with substrate material of quartz. In addition, this paper will give some useful information to optics related researchers and engineers. For example, the microlenses (micro-diffractive lens, micro-grating, etc.) can be directly integrated together with top-end of optical fibers working in near infrared region via FIB milling [13]. The discussion regarding the optical properties after the FIB milling will be helpful for the fiber system engineers to take these factors into consideration when they design their related systems.

**ACKNOWLEDGEMENTS** This work was supported in part by the Funding for Strategic Research Program on Ultra-Precision Engineering from the A-STAR (Agency of Science Technology and Research, Singapore), and Innovation in Manufacturing Systems and Technology (IMST) Singapore–Massachusetts Institute of Technology (MIT) Alliance. The authors thank Mrs. Xie Hong for her enthusiastic help of measuring the refractive index of the quartz before and after the FIB processing, Ms. Qian Haixia for her help for measurement of XRD, and Dr. Wei Xing Yu for his measurement of transmission for my samples.

## REFERENCES

1 Y. Fu, N.K.A. Bryan, Opt. Express **7**, 141 (2000)
2 Y. Fu, N.K.A. Bryan, Appl. Opt. **40**, 5872 (2001)
3 Y. Fu, N.K.A. Bryan, Opt. Express **12**, 227 (2004)
4 Y. Fu, N.K.A. Bryan, IEEE Photonics Technol. Lett. **13**, 424 (2001)
5 Y. Fu, N.K.A. Bryan, Opt. Eng. **40**, 511 (2001)
6 Y. Fu, N.K.A. Bryan, W. Zhou, Opt. Express **12**, 1803 (2004)
7 J. Melngailis, J. Vac. Sci. Technol. B **5**(2), 469 (1987)
8 Commonly used software for simulation and analysis of ion beam processing. Available at http://www.srim.org/srim/srimlegl.h
9 E.D. Palik (ed.), *Handbook of Optical Constants of Solids* (Academic, New York, 1985)
10 J.C. Pivin, M. Sendova, M. Nikolaeva, D. Dimova-Malinovska, A. Martucci, Appl. Phys. A **75**, 401 (2002)
11 U. Kriebig, M. Vollmer, *Optical Properties of Metal Clusters*, Springer Ser. Mater. Sci., vol 25 (Springer, Berlin Heidelberg New York, 1996)
12 M.A. Garcia, J. Llpois, S.E. Paje, Chem. Phys. Lett. **315**, 313 (1999)
13 Y. Fu, N.K.A. Bryan, *Holography, Diffractive Optics and Applications II*. SPIE Proc., vol 5636 (in press)